Inorg. Chem. **2008**, *47*, 9256−9264

Highly Selective Phosphorescent Chemosensor for Fluoride Based on an Iridium(III) Complex Containing Arylborane Units

Qiang Zhao,[†] Fuyou Li,[*,†] Shujuan Liu,[‡] Mengxiao Yu,[†] Zhiqiang Liu,[†,§] Tao Yi,[†] and Chunhui Huang[†]

Department of Chemistry & Laboratory of Advanced Materials, Fudan University, Shanghai 200433, People's Republic of China, and Institute of Advanced Materials (IAM), Nanjing University of Posts & Telecommunications, Nanjing 210003, People's Republic of China

Received March 19, 2008

A new phosphorescent iridium(III) complex $[Ir(Bpq)_2(bpy)]^+PF_6^-$ based on cyclometalated ligands (Bpq) containing a dimesitylboryl group was synthesized and characterized by photophysical and electrochemical studies. The excited-state properties of Bpq and $[Ir(Bpq)_2(bpy)]^+PF_6^-$ were investigated using molecular orbital calculations. Importantly, both Bpq and $[Ir(Bpq)_2(bpy)]^+PF_6^-$ could be used as highly selective chemosensors for a fluoride anion (F^-) detected by the naked eye, owing to the interaction of the dimesitylboryl group ($BMes_2$) with F^-. For the Bpq ligand, a red shift of the emission spectrum was observed upon the addition of F^-, which could be attributed to an excited-state switch from a $\pi-\pi^*$ transition to a charge-transfer transition upon complexation with F^-. The addition of F^- to a solution of $[Ir(Bpq)_2(bpy)]^+PF_6^-$ induced a change in the solution color from yellow to orange-red and phosphorescent quenching, indicating that $[Ir(Bpq)_2(bpy)]^+PF_6^-$ could act as an excellent ON−OFF-type phosphorescent chemosensor for F^-.

Introduction

Fluoride anion (F^-), the smallest anion, plays an essential role in a broad range of biological, medical, and chemical processes and in applications such as dental care, treatment of osteoporosis, fluorination of water supplies, and even chemical and nuclear warfare agents.[1] As a result, its recognition and detection are of growing interest, and there is a need to develop new selective and sensitive methods for fluoride detection in various environments. Up to now, a large number of synthetic chromophores have been designed as chemosensors for this important analyte.[2] It is well-known that (thio)ureas,[2] amides,[3] pyrrole,[4] and imidazolium[5] are particularly effective in reacting with F^- through the formation of a hydrogen bond between the active N−H group and F^-. Recently, specific Lewis acid−base interactions, such as the strong affinity of a boron atom toward F^-,

* To whom correspondence should be addressed. E-mail: fyli@fudan.edu.cn. Tel: 86-21-55664185. Fax: 86-21-55664621.
† Fudan University.
‡ Nanjing University of Posts and Telecommunications.
§ Permanent address: Shandong University, Jinan 250100, People's Republic of China.

(1) (a) Kirk, K. L. *Biochemistry of the Halogens and Inorganic Halides*; Plenum Press: New York, 1991; p 58. (b) Riggs, B. L. *Bone and Mineral Research*; Annual 2; Elsevier: Amsterdam, The Netherlands, 1984; p 366. (c) Wiseman, A. *Handbook of Experimental Pharmacology XX/2*; Springer-Verlag: Berlin, 1970; Part 2, p 48.

(2) For recent reviews on anion receptors, see: (a) *Coord. Chem. Rev.* **2003**, *240*,issues 1 and 2 (Special Issues on anion receptors). (b) Martínez-Máñez, R.; Sancenón, F. *Chem. Rev.* **2003**, *103*, 4419–4476. (c) Suksai, C.; Tuntulani, T. *Chem. Soc. Rev.* **2003**, *32*, 192–202. (d) Best, M. D.; Tobey, S. L.; Anslyn, E. V. *Coord. Chem. Rev.* **2003**, *240*, 3–15. (e) Beer, P. D.; Gale, P. A. *Angew. Chem., Int. Ed.* **2001**, *40*, 486–516. (f) Snowden, T. S.; Anslyn, E. V. *Curr. Opin. Chem. Biol.* **1999**, 740–746. (g) Arnendola, V.; Bonizzoni, M.; Esteban-Gomez, D.; Fabbrizzi, L.; Licchelli, M.; Sancenon, F.; Taglietti, A. *Coord. Chem. Rev.* **2006**, *250*, 1451–1470. (h) Gunnlaugsson, T.; Glynn, M.; Tocci, G. M.; Kruger, P. E.; Pfeffer, F. M. *Coord. Chem. Rev.* **2006**, *250*, 3094–3117. (i) Amendola, V.; Esteban-Gomez, D.; Fabbrizzi, L.; Licchelli, M. *Acc. Chem. Res.* **2006**, *39*, 343–353.

(3) For example, see: (a) Gale, P. A. *Acc. Chem. Res.* **2006**, *39*, 465–475. (b) Bondy, C. R.; Loeb, S. J. *Coord. Chem. Rev.* **2003**, *240*, 77–99.

(4) (a) Sessler, J. L.; Camiolo, S.; Gale, P. A. *Coord. Chem. Rev.* **2003**, *240*, 17–55. (b) Plitt, P.; Gross, D. E.; Lynch, V. M.; Sessler, J. L. *Chem.—Eur. J.* **2007**, *13*, 1374–1381. (c) Lin, C. I.; Selvi, S.; Fang, J. M.; Chou, P. T.; Lai, C. H.; Cheng, Y. M. *J. Org. Chem.* **2007**, *72*, 3537–3542. (d) de Namor, A. F. D.; Shehab, M.; Abbas, I.; Withams, M. V.; Zvietcovich-Guerra, J. *J. Phys. Chem. B* **2006**, *110*, 12653–12659.

(5) Yoon, J. Y.; Kim, S. K.; Singh, N. J.; Kim, K. S. *Chem. Soc. Rev.* **2006**, *35*, 355–360.

(6) (a) Yamaguchi, S.; Akiyama, S.; Tamao, K. *J. Am. Chem. Soc.* **2001**, *123*, 11372–11375. (b) Yamaguchi, S.; Akiyama, S.; Tamao, K. *J. Am. Chem. Soc.* **2000**, *122*, 6335–6336. (c) Yamaguchi, S.; Shirasaka, T.; Akiyama, S.; Tamao, K. *J. Am. Chem. Soc.* **2002**, *124*, 8816–8817. (d) Kubo, Y.; Yamamoto, M.; Ikeda, M.; Takeuchi, M.; Shinkai, S.; Yamaguchi, S.; Tamao, K. *Angew. Chem., Int. Ed.* **2003**, *42*, 2036–2040.

10.1021/ic800500c CCC: $40.75
Published on Web 09/24/2008

have been adopted as an efficient approach for fluoride detection.[6−11] Some three-coordinated boron compounds with a donor−π conjugation−acceptor (D−π−A) chemical structure,[12] in which the dimesitylboryl ($BMes_2$) group was adopted as the electron acceptor, were reported to be highly selective colorimetric chemosensors. In the presence of F^-, strong B−F interaction can interrupt the extended π conjugation of these organoboron derivatives, thereby causing a dramatic change in the photophysical properties. To the best of our knowledge, however, the output signals of most fluoride chemosensors are limited to absorption and fluorescence signals. Recently, Gabbai et al. reported the first example of a phosphorescent anion sensor based on a heteronuclear B/Hg bidentate Lewis acid.[7a]

Recently, the use of phosphorescent heavy-metal complexes as chemosensors has attracted considerable interest because of advantageous photophysical properties of heavy-metal complexes, such as emission colors shifts with changes in the local environment, significant Stokes shifts for easy separation of excitation and emission, and relatively long lifetimes compared to purely organic luminophores. Especially, the long lifetime of phosphorescence can eliminate the interference of the short-lifetime background fluorescence and scattering light by using a time-resolved luminescence technology. The selectivity is enhanced because it is a less usual phenomenon than that of fluorescence. Importantly, the long lifetime also allows the excited state ample time to sample its environment, and it is this interaction that makes these materials sensitive reporters. Some complexes, such as platinum(II), rhenium(I), and ruthenium(II) complexes, have been successfully utilized as phosphorescent chemosensors for anions,[13] oxygen concentration,[14] and metal ions.[15] As one of the best classes of phosphorescent dyes,[16−25] iridium(III) complexes exhibited tunable luminescent color (from blue to red), high luminescent quantum yield (~0.7 in organic solvent), and remarkable structure−function relationships and have been used as highly efficient electroluminescent emitters in organic light-emitting diodes. Recently, the photophysical properties of iridium(III) complexes were reported to be affected by external stimuli such

(7) (a) Melaimi, M.; Gabbai, F. P. *J. Am. Chem. Soc.* **2005**, *127*, 9680–9681. (b) Sole, S.; Gabbai, F. P. *Chem. Commun.* **2004**, 1284–1285. (c) Lee, M. H.; Agou, T.; Kobayashi, J.; Kawashima, T.; Gabbai, F. P. *Chem. Commun.* **2007**, 1133–1135. (d) Chiu, C. W.; Gabbai, F. P. *J. Am. Chem. Soc.* **2006**, *128*, 14248–14249. (e) Hudnall, T. W.; Melaimi, M.; Gabbai, F. P. *Org. Lett.* **2006**, *8*, 2747–2749. (f) Hudnall, T. W.; Gabbaı, F. P. *J. Am. Chem. Soc.* **2007**, *129*, 11978–11986.

(8) (a) Liu, X. Y.; Bai, D. R.; Wang, S. *Angew. Chem., Int. Ed.* **2006**, *45*, 5475–5478. (b) Bai, D. R.; Liu, X. Y.; Wang, S. *Chem.—Eur. J.* **2007**, *13*, 5713–5723. (c) Sun, Y.; Ross, N.; Zhao, S. B.; Huszarik, K.; Jia, W. L.; Wang, R. Y.; Macartney, D.; Wang, S. *J. Am. Chem. Soc.* **2007**, *129*, 7510–7511. (d) Zhao, S. B.; McCormick, T.; Wang, S. *Inorg. Chem.* **2007**, *46*, 10965–10967.

(9) (a) Liu, Z. Q.; Shi, M.; Li, F. Y.; Fang, Q.; Chen, Z. H.; Yi, T.; Huang, C. H. *Org. Lett.* **2005**, *7*, 5481–5484. (b) Zhou, Z. G.; Xiao, S. Z.; Xu, J.; Liu, Z. Q.; Shi, M.; Li, F. Y.; Yi, T.; Huang, C. H. *Org. Lett.* **2006**, *8*, 3911–3914. (c) Zhou, Z. G.; Yang, H.; Shi, M.; Xiao, S. Z.; Li, F. Y.; Yi, T.; Huang, C. H. *ChemPhysChem* **2007**, *8*, 1289–1292. (d) Zhou, Z. G.; Li, F. Y.; Yi, T.; Huang, C. H. *Tetrahedron Lett.* **2007**, *48*, 6633–6636.

(10) (a) Dusemund, C.; Sandanayake, K. R. A. S.; Shinkai, S. *J. Chem. Soc., Chem. Commun.* **1995**, 333–334. (b) Yamamoto, H.; Ori, A.; Ueda, K.; Dusemund, C.; Shinkai, S. *Chem. Commun.* **1996**, 407–408.

(11) (a) Shiratori, H.; Ohno, T.; Nozaki, K.; Osuka, A. *Chem. Commun.* **1999**, 2181–2182. (b) Sundararaman, A.; Victor, M.; Varughese, R.; Jäkle, F. *J. Am. Chem. Soc.* **2005**, *127*, 13748–13749. (c) Aldridge, S.; Bresner, C.; Fallis, I. A.; Coles, S. J.; Hursthouse, M. B. *Chem. Commun.* **2002**, 740–741. (d) Badugu, R.; Lakowicz, J. R.; Geddes, C. D. *Curr. Anal. Chem.* **2005**, *1*, 157. (e) Bresner, C.; Day, J. K.; Coombs, N. D.; Fallis, I. A.; Aldridge, S.; Coles, S. J.; Hursthouse, M. B. *Dalton Trans.* **2006**, 3660–3667. (f) Bresner, C.; Aldridge, S.; Fallis, I. A.; Jones, C.; Ooi, L.-L. *Angew. Chem., Int. Ed.* **2005**, *44*, 3606–3609. (g) Cooper, C. R.; Spencer, N.; James, T. D. *Chem. Commun.* **1998**, 1365–1366. (h) Arimori, S.; Davidson, M. G.; Fyles, T. M.; Hibbert, T. G.; James, T. D.; Kociok-Koehn, G. I. *Chem. Commun.* **2004**, 1640–1641. (i) DiCesare, N.; Lakowicz, J. R. *Anal. Biochem.* **2002**, *301*, 111–116. (j) Parab, K.; Venkatasubbaiah, K.; Jäkle, F. *J. Am. Chem. Soc.* **2006**, *128*, 12879–12885. (k) Williams, V. C.; Piers, W. E.; Clegg, W.; Elsegood, M. R. J.; Collins, S.; Marder, T. B. *J. Am. Chem. Soc.* **1999**, *121*, 3244–3245. (l) Agou, T.; Kobayashi, J.; Kawashima, T. *Org. Lett.* **2005**, *7*, 4373–4376. (m) Sakuda, E.; Funahashi, A.; Kitamura, N. *Inorg. Chem.* **2006**, *45*, 10670–10677. (n) Oehlke, A.; Auer, A. A.; Jahre, I.; Walfort, B.; Rüffer, T.; Zoufalá, P.; Lang, H.; Spange, S. *J. Org. Chem.* **2007**, *72*, 4328–4339.

(12) (a) Entwistle, C. D.; Marder, T. B. *Chem. Mater.* **2004**, *16*, 4574–4585. (b) Entwistle, C. D.; Marder, T. B. *Angew. Chem., Int. Ed.* **2002**, *41*, 2927–2931. *Angew. Chem.* **2002**, *114*, 3051−3056. (c) Yuan, Z.; Entwistle, C. D.; Collings, J. C.; Albesa-Jové, D.; Batsanov, A. S.; Howard, J. A. K.; Taylor, N. J.; Kaiser, H. M.; Kaufmann, D. E.; Poon, S.-Y.; Wong, W.-Y.; Jardin, C.; Fathallah, S.; Boucekkine, A.; Halet, J.-F.; Marder, T. B. *Chem.—Eur. J.* **2006**, *12*, 2758–2771. (d) Huh, J. O.; Do, Y.; Lee, M. H. *Organometallics* **2008**, *27*, 1022–1025.

(13) (a) Anzenbacher, P., Jr.; Tyson, D. S.; Jursıkova, K.; Castellano, F. N. *J. Am. Chem. Soc.* **2002**, *124*, 6232–6233. (b) Fillaut, J.-L.; Andries, J.; Perruchon, J.; Desvergne, J.-P.; Toupet, L.; Fadel, L.; Zouchoune, B.; Saillard, J.-Y. *Inorg. Chem.* **2007**, *46*, 5922–5932. (c) Jose, D. A.; Kar, P.; Koley, D.; Ganguly, B.; Thiel, W.; Ghosh, H. N.; Das, A. *Inorg. Chem.* **2007**, *46*, 5576–5584.

(14) (a) Huynh, L.; Wang, Z.; Yang, J.; Stoeva, V.; Lough, A.; Manners, I.; Winnik, M. A. *Chem. Mater.* **2005**, *17*, 4765–4773. (b) Briñas, R. P.; Troxler, T.; Hochstrasser, R. M.; Vinogradov, S. A. *J. Am. Chem. Soc.* **2005**, *127*, 11851–11862. (c) Han, B.-H.; Winnik, M. A. *Chem. Mater.* **2005**, *17*, 4001–4009. (d) McGee, K. A.; Veltkamp, D. J.; Marquardt, B. J.; Mann, K. R. *J. Am. Chem. Soc.* **2007**, *129*, 15092–15093. (e) Lei, B.; Li, B.; Zhang, H.; Zhang, L.; Li, W. *J. Phys. Chem. C* **2007**, *111*, 11291–11301.

(15) Tang, W. S.; Lu, X. X.; Wong, K. M. C.; Yam, V. W. W. *J. Mater. Chem.* **2005**, *15*, 2714–2720.

(16) For recent review, see: (a) Chou, P. T.; Chi, Y. *Chem.—Eur. J.* **2007**, *13*, 380–395. (b) Ma, B.; Djurovich, P. I.; Thompson, M. E. *Coord. Chem. Rev.* **2005**, *249*, 1501–1510. (c) Forrest, S. R.; Thompson, M. E. *Chem. Rev.* **2007**, *107*, 923–925. (d) Huang, C. H.; Li, F. Y.; Huang, W. *Introduction to Organic Light-Emitting Materials and Devices*; Press of Fudan University: Shanghai, China, 2005. (e) Grushin, V. V. *Chem, Rev.* **2004**, *104*, 1629–1662.

(17) Sprouse, S.; King, K. A.; Spellane, P. J.; Watts, R. J. *J. Am. Chem. Soc.* **1984**, *106*, 6647–6653.

(18) (a) Lamansky, S.; Djurovich, P.; Murphy, D.; Abdel-Razzaq, F.; Kwong, R.; Tsyba, I.; Bortz, M.; Mui, B.; Bau, R.; Thompson, M. E. *Inorg. Chem.* **2001**, *40*, 1704–1711. (b) Tamayo, A. B.; Garon, S.; Sajoto, T.; Djurovich, P. I.; Tsyba, I. M.; Bau, R.; Thompson, M. E. *Inorg. Chem.* **2005**, *44*, 8723–8732. (c) Lo, S.-C.; Anthopoulos, T. D.; Namdas, E. B.; Burn, P. L.; Samuel, I. D. W. *Adv, Mater.* **2005**, *17*, 1945–1948. (d) Lo, S.-C.; Richards, G. J.; Markham, P. J.; Namdas, E. B.; Sharma, S.; Burn, P. L.; Samuel, I. D. W. *Adv. Funct. Mater.* **2005**, *15*, 1451–1458. (e) Bettington, S.; Tavasli, M.; Bryce, M. R.; Beeby, A.; Al-Attar, H. A.; Monkman, A. P. *Chem.—Eur. J.* **2007**, *13*, 1423–1431. (f) King, S. M.; Al-Attar, H. A.; Evans, R. J.; Congreve, A.; Beeby, A.; Monkman, A. P. *Adv. Funct. Mater.* **2006**, *16*, 1043–1050. (g) Zhou, G.; Ho, C. L.; Wong, W. Y.; Wang, Q.; Ma, D.; Wang, L.; Lin, Z.; Marder, T. B.; Beeby, A. *Adv. Funct. Mater.* **2008**, *18*, 499–511.

(19) (a) Slinker, J. D.; Gorodetsky, A. A.; Lowry, M. S.; Wang, J.; Parker, S.; Rohl, R.; Bernhard, S.; Malliaras, G. G. *J. Am. Chem. Soc.* **2004**, *126*, 2763–2767. (b) Lowry, M. S.; Bernhard, S. *Chem.—Eur. J.* **2006**, *12*, 7970–7977.

(20) (a) Yeh, S.-J.; Wu, M.-F.; Chen, C.-T.; Song, Y.-H.; Chi, Y.; Ho, M.-H.; Hsu, S.-F.; Chen, C. H. *Adv. Mater.* **2005**, *17*, 285–289. (b) Yang, C.-H.; Li, S.-W.; Chi, Y.; Cheng, Y.-M.; Yeh, Y.-S.; Chou, P.-T.; Lee, G.-H.; Wang, C.-H.; Shu, C.-F. *Inorg. Chem.* **2005**, *44*, 7770–7780.

as biomolecules (such as estrogen receptor α)[24] and chemical compounds (such as anions, alkali cations, and amino acid).[26] Up to now, however, only a few examples have been reported of iridium(III) complexes used as chemosensors to selectively sense heavy-metal ions such as Hg^{2+} or Pb^{2+} over other metal cations with high sensitivity.[27]

It is well-known that the photophysical and electrochemical properties of iridium(III) complexes are dependent on the chemical structures of cyclometalated ligands (C∧N ligands). When a cyclometalated ligand of an iridium(III) complex contains a specific coordinating element for an analyte, the presence of this analyte can lead to dramatic changes in the photophysical and electrochemical properties of the iridium(III) complex. In the present study, on the basis of the strong interaction between the three-coordination boron atom and F^-, a $BMes_2$ group was introduced into a cyclometalated ligand (Bpq), and a novel iridium(III) complex salt $[Ir(Bpq)_2(bpy)]^+PF_6^-$ based on Bpq (see Scheme 1) was synthesized. The photophysical and elelctrochemical properties of Bpq and $[Ir(Bpq)_2(bpy)]^+PF_6^-$ have been investigated and compared with those of a model complex salt $[Ir(pq)_2(bpy)]^+PF_6^-$ without the $BMes_2$ group. Importantly, further investigation shows that $[Ir(Bpq)_2(bpy)]^+PF_6^-$ can act as a highly selective phosphorescent chemosensor for F^-.

Scheme 1. Chemical Structures of Ligand and Iridium(III) Complexes

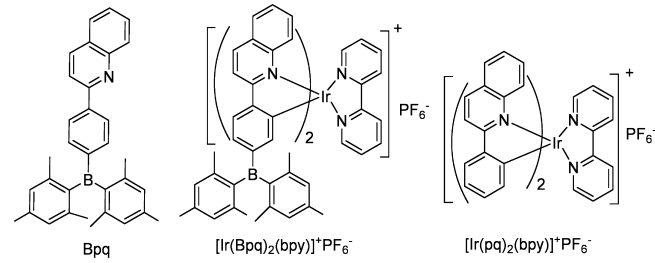

Experimental Section

Materials. Acetylacetone, dimesitylboron fluoride, and 2-ethoxyethanol were obtained from Acros. 2-Aminobenzaldehyde, acetophenone, 2,2-bipyridine, 4-bromoacetophenone, $IrCl_3 \cdot 3H_2O$, and $Pd(PPh_3)_4$ were industrial products and were used without further purification.

General Experiments. ^1H NMR spectra were recorded with a Varian spectrometer at 400 MHz. Mass spectra were obtained on a Shimadzu matrix-assisted laser desorption/ionization time-of-flight mass spectrometer (MALDI-TOF-MS). The UV−visible spectra were recorded on a Shimadzu UV-2550 spectrometer. Steady-state emission experiments at room temperature were measured on an Edinburgh FLS 920 spectrometer. Lifetime studies were performed with an Edinburgh FLS 920 photocounting system with a hydrogen-filled pulse lamp as the excitation source. The data were analyzed by iterative convolution of the luminescence decay profile with the instrument response function using the software package provided by Edinburgh Instruments. Quantum yields were determined with a Hamamatsu C9920-01 calibrated integrating sphere system. The solution was degassed by three freeze−pump−thaw cycles.

Calculation of Binding Constants. The binding constant (K) of Bpq with F^- was calculated from the flowing equation $A_0/(A - A_0) = [a/(b - a)][(1/K[F^-]) + 1]$,[28a] where A_0 and A are the absorbances at 333 nm in the absence and presence of F^-, respectively. In addition, $a = \epsilon_L \lambda_{exc} (d\Phi_L/d\lambda)_{\lambda_{em}} \Delta\lambda$ and $b = \epsilon_{ML} \lambda_{exc} (d\Phi_{ML}/d\lambda)_{\lambda_{em}} \Delta\lambda$, where $\Delta\lambda$ is the band pass of the emission monochromator, L and ML refer to Bpq before and after binding with F^-, respectively, Φ_L and Φ_{ML} are the respective quantum yields of these two species, and ϵ_L and ϵ_{ML} are the corresponding molar absorption coefficients. The binding constant of $[Ir(Bpq)_2(bpy)]^+PF_6^-$ with F^- was calculated from the absorption titration data by using the *Hyperquad2006* program.[28b]

Electrochemical Measurements. Electrochemical measurements were performed with an Eco Chemie's Autolab. All measurements were carried out in a one-compartment cell under nitrogen gas, equipped with a glassy-carbon working electrode, a platinum wire counter electrode, and an Ag/Ag^+ reference electrode. The supported electrolyte was a 0.10 mol L^{-1} dichloromethane solution of tetrabutylammonium hexafluorophosphate (Bu_4NPF_6). The scan rate was 50 mV s^{-1}.

(21) (a) Zhao, Q.; Jiang, C.-Y.; Shi, M.; Li, F.-Y.; Yi, T.; Cao, Y.; Huang, C.-H. *Organometallics* **2006**, *25*, 3631–3638. (b) Zhao, Q.; Liu, S.; Shi, M.; Wang, C.; Yu, M.; Li, L.; Li, F.; Yi, T.; Huang, C. *Inorg. Chem.* **2006**, *45*, 6152–6160. (c) Liu, S. J.; Zhao, Q.; Chen, R. F.; Deng, Y.; Fan, Q. L.; Li, F. Y.; Wang, L. H.; Huang, C. H.; Huang, W. *Chem.—Eur. J.* **2006**, *12*, 4351–4361. (d) Liu, Z. W.; Guan, M.; Bian, Z. Q.; Nie, D. B.; Gong, Z. L.; Li, Z. B.; Huang, C. H. *Adv. Funct. Mater.* **2006**, *16*, 1441–1448. (e) Li, X. H.; Chen, Z.; Shen, L.; Li, F. Y.; Zhao, Q.; Yi, T.; Cao, Y.; Huang, C. H. *Inorg. Chem.* **2007**, *46*, 5518–5527. (f) Liu, S. J.; Zhao, Q.; Deng, Y.; Xia, Y. J.; Lin, J.; Fan, Q. L.; Wang, L. H.; Huang, W. *J. Phys. Chem. C* **2007**, *111*, 1166–1175. (g) Zhao, Q.; Li, L.; Li, F. Y.; Yu, M. X.; Liu, Z. P.; Yi, T.; Huang, C. H. *Chem. Commun.* **2008**, 685–687. (h) Yu, M. X.; Zhao, Q.; Shi, L. X.; Li, F. Y.; Zhou, Z. G.; Yang, H.; Yi, T.; Huang, C. H. *Chem. Commun.* **2008**, 2115–2117.

(22) (a) Jiang, J. X.; Xu, Y. H.; Yang, W.; Guan, R.; Liu, Z. Q.; Zhen, H. Y.; Cao, Y. *Adv. Mater.* **2006**, *18*, 1769–1773. (c) Chen, L. Q.; You, H.; Yang, C. L.; Ma, D. G.; Qin, J. Q. *Chem. Commun.* **2007**, 1352–1354. (c) Rehmann, N.; Ulbricht, C.; Köhnen, A.; Zacharias, P.; Gather, M. C.; Hertel, D.; Holder, E.; Meerholz, K.; Schubert, U. S. *Adv. Mater.* **2008**, *20*, 129–133. (d) Liu, S. J.; Zhao, Q.; Fan, Q. L.; Huang, W. *Eur. J. Inorg. Chem.* **2008**, 2177–2185. (e) You, Y.; Seo, J.; Kim, S. H.; Kim, K. S.; Ahn, T. K.; Kim, D.; Park, S. Y. *Inorg. Chem.* **2008**, *47*, 1476–1487.

(23) Coppo, P.; Duati, M.; Kozhevnikov, V. N.; Hofstraat, J. W.; De Cola, L. *Angew. Chem.* **2005**, *117*, 1840–1844. *Angew. Chem., Int. Ed.* **2005**, *44*, 1806−1810.

(24) (a) Lo, K. K.-W.; Chung, C.-K.; Zhu, N. *Chem.—Eur. J.* **2003**, *9*, 475–483. (b) Lo, K. K.-W.; Chan, J. S.-W.; Lui, L.-H.; Chung, C.-K. *Organometallics* **2004**, *23*, 3108–3116. (c) Lo, K. K.-W.; Li, C.-K.; Lau, J. S.-Y. *Organometallics* **2005**, *24*, 4594–4601. (d) Lo, K. K.-W.; Chung, C.-K.; Zhu, N. *Chem.—Eur. J.* **2006**, *12*, 1500–1512. (e) Lo, K. K. W.; Lau, J. S. Y. *Inorg. Chem.* **2007**, *46*, 700–709. (f) Lo, K. K.-W.; Zhang, K. Y.; Chung, C.-K.; Kwok, K. Y. *Chem.—Eur. J.* **2007**, *13*, 7110–7120. (g) Lo, K. K. W; Hui, W. K.; Chung, C. K.; Tsang, K. H. K.; Lee, T. K. M.; Li, C. K.; Lau, J. S. Y.; Ng, D. C. M. *Coord. Chem. Rev.* **2006**, *250*, 1724–1736.

(25) (a) Yersin, H. *Top. Curr. Chem.* **2004**, *241*, 1–6. (b) You, Y. M.; Park, S. Y. *J. Am. Chem. Soc.* **2005**, *127*, 12438–12439. (c) Tsuboyama, A.; Iwawaki, H.; Furugori, M.; Mukaide, T.; Kamatani, J.; Igawa, S.; Moriyama, T.; Miura, S.; Takiguchi, T.; Okada, S.; Hoshino, M.; Ueno, K. *J. Am. Chem. Soc.* **2003**, *125*, 12971–12979. (d) Polson, M.; Ravaglia, M.; Fracasso, S.; Garavelli, M.; Scandola, F. *Inorg. Chem.* **2005**, *44*, 1282–1289. (e) Obara, S.; Itabashi, M.; Okuda, F.; Tamaki, S.; Tanabe, Y.; Ishii, Y.; Nozaki, K.; Haga, M. *Inorg. Chem.* **2006**, *45*, 8907–8921. (f) Wilkinson, A. J.; Puschmann, H.; Howard, J. A. K.; Foster, C. E.; Williams, J. A. G. *Inorg. Chem.* **2006**, *45*, 8685–8699.

(26) (a) Ho, M. L.; Hwang, F. M.; Chen, P. N.; Hu, Y. H.; Cheng, Y. M.; Chen, K. S.; Lee, G. H.; Chi, Y.; Chou, P. T. *Org. Biomol. Chem.* **2006**, *4*, 98–103. (b) Goodall, W.; Williams, J. A. G. *J. Chem. Soc., Dalton Trans.* **2000**, 2893–2895. (c) Zhao, Q.; Liu, S. J.; Shi, M.; Li, F. Y.; Jing, H.; Yi, T.; Huang, C. H. *Organometallics* **2007**, *26*, 5922–5930. (d) Chen, H. L.; Zhao, Q.; Li, F. Y.; Wu, Y. B.; Yang, H.; Yi, T.; Huang, C. H. *Inorg. Chem.* **2007**, *46*, 11075–11081.

(27) (a) Zhao, Q.; Cao, T. Y.; Li, F. Y.; Li, X. H.; Jing, H.; Yi, T.; Huang, C. H. *Organometallics* **2007**, *26*, 2077–2081. (b) Ho, M. L.; Cheng, Y. M.; Wu, L. C.; Chou, P. T.; Lee, G. H.; Hsu, F. C.; Chi, Y. *Polyhedron* **2007**, *26*, 4886–4892. (c) Zhao, Q.; Liu, S. J.; Li, F. Y.; Yi, T.; Huang, C. H. *Dalton Trans.* **2008**, 3836–3840.

Scheme 2. Synthesis of Ligand Bpq[a] and of Complex $[Ir(Bpq)_2(bpy)]^+PF_6^-$[b]

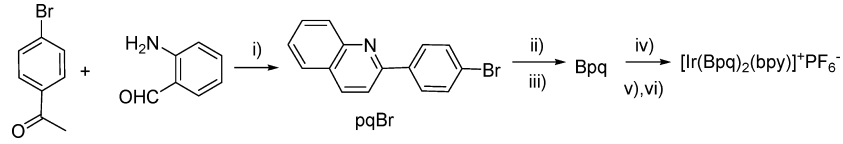

[a] (i) NaOH, ethanol, reflux; (ii) nBuLi, THF, −78 °C; (iii) Mes2BF, THF, −78 °C. [b] (iv) 2-Ethoxyethanol:H_2O = 3:1, 110 °C, N_2; (v) bipyridine, CH_2Cl_2, reflux; (vi) KPF6, RT.

Theoretical Calculations. The calculation was performed using the *Gaussian 03* suite of programs.[29] The optimizations of the ligand and complex structures were performed using B3LYP density functional theory (DFT). The LANL2DZ basis set was used to treat the iridium atom, whereas the 6-31G* basis set was used to treat all other atoms. The contours of the highest occupied molecular and lowest unoccupied molecular orbitals (HOMOs and LUMOs) were plotted.

Synthesis of pqBr. To a mixture of 4-bromoacetophenone (4.0 mmol) and 2-aminobenzadehyde (4 mmol) in ethanol was added saturated ethanolic NaOH, and the mixture was refluxed overnight (see Scheme S1 in the Supporting Information). After cooling, the precipitate was collected by filtration and recrystallized from a CH_2Cl_2 solution to obtain white crystals (2.8 mmol) in 70% yield. ^{1}H NMR (400 MHz, $CDCl_3$, 298 K): δ 8.23 (d, 1H), 9.13 (d, 1H), 8.04 (d, 2H), 7.82−7.85 (m, 2H), 7.73 (t, 1H), 7.64 (d, 2H), 7.54 (t, 1H). Anal. Calcd for $C_{15}H_{10}NBr$: C, 63.40; H, 3.55; N, 4.93. Found: C, 63.72; H, 3.34; N, 4.55.

Synthesis of Bpq. Under a nitrogen atmosphere, *n*-butyllithium (1.32 mL, 2.11 mmol, 1.6 M in *n*-hexane) was added dropwise to a stirred solution of Brpq (0.500 g, 1.76 mmol) in absolute tetrahydrofuran (THF; 18 mL) at −78 °C. The reaction mixture was stirred for 1 h at −78 °C, and then a solution of dimesitylboron fluoride (0.566 g, 2.11 mmol) in THF was added (see Scheme 2). After stirring for 18 h at room temperature, the reaction mixture was quenched with H_2O (50 mL) and extracted three times with CH_2Cl_2 (50 mL). The combined organic extracts were dried over Na_2SO_4, and the solvent was removed in vacuo. The crude product was purified by chromatography with CH_2Cl_2/petroleum ether (1:4) to obtain white needles in 60% yield. ^{1}H NMR (400 MHz, $CDCl_3$, 298 K): δ 8.13−8.25 (m, 4H), 7.54−7.93 (m, 6H), 6.85 (s, 4H), 2.33 (s, 6H), 2.05 (s, 12H). Anal. Calcd for $C_{33}H_{32}NB$: C, 87.41; H, 7.11; N, 3.09. Found: C, 87.79; H, 7.55; N, 3.52.

Synthesis of $[Ir(Bpq)_2(bpy)]^+PF_6^-$. A mixture of 2-ethoxyethanol and water (3:1, v/v) was added to a flask containing $IrCl_3 \cdot 3H_2O$ (1 mmol) and Bpq (2.5 mmol). The mixture was refluxed for 24 h. After cooling, the orange solid precipitate was filtered to give crude cyclometalated iridium(III) chloro-bridged dimer. The solution of cyclometalated iridium(III) chloro-bridged dimer (0.079 mmol) and bpy (0.158 mmol) in CH_2Cl_2/MeOH [30 mL, 2:1 (v/v)] was heated to reflux. After 4 h, the red solution was cooled to room temperature and then a 10-fold excess of potassium hexafluorophosphate was added. The suspension was stirred for 2 h and then was filtered to remove insoluble inorganic salts. The solution was evaporated to dryness under reduced pressure. It was chromatographed by using CH_2Cl_2/acetone (15:1) to afford an orange-yellow solid in 70% yield. ^{1}H NMR (400 MHz, $CDCl_3$, 298 K): δ 8.36 (d, 2H), 8.11 (d, 2H), 8.00 (t, 2H), 7.90−7.96 (m, 4H), 7.82 (d, 2H), 7.58 (d, 2H), 7.32−7.39 (m, 4H), 7.24 (d, 2H), 7.10 (d, 2H), 6.95 (t, 2H), 6.48 (s, 8H), 6.24 (s, 2H), 2.24 (s, 12H), 1.62 (s, 24H). Anal. Calcd for $IrC_{76}H_{70}B_2F_6N_4P$: C, 65.28; H, 5.05; N, 4.01. Found: C, 65.68; H, 5.46; N, 4.45. MS (MALDI-TOF): *m/e* 1254.0 (M − PF_6).

Results and Discussion

Synthesis. The synthesis procedure for Bpq and $[Ir(Bpq)_2(bpy)]^+PF_6^-$ is outlined in Scheme 2. The precursor pqBr (Scheme 2) was easily obtained in good yield by a Friedländer condensation reaction of 2-aminobenzadehyde with 4-bromoacetophenone according to a previously published procedure.[30] Ligand Bpq was synthesized in 60% yield by lithiating pqBr, followed by the addition of Mes_2BF at −78 °C.[31] The bis-cyclometalated iridium(III) complex salt $[Ir(Bpq)_2(bpy)]^+PF_6^-$ containing bipyridine (bpy) and the Bpq ligand with the $BMes_2$ group were prepared by a two-step reaction via iridium(III) μ-chloro-bridged dimer complexes according to a conventional procedure.[32] The dinuclear cyclometalated iridium(III) chloro-bridged precursor $[Ir(Bpq)_2Cl]_2$ was synthesized using the same methods as those reported by Nonoyama.[33] By bridge splitting reactions of $[Ir(Bpq)_2Cl]_2$ and subsequent complexation with 2,2-bipyridine, $[Ir(Bpq)_2(bpy)]^+PF_6^-$ was synthesized in a yield of 70% and characterized by elemental analysis, ^{1}H NMR spectroscopy, and MALDI-TOF-MS spectroscopy.

Photophysical and Electrochemical Properties of Bpq. Data on the UV−vis absorption and photoluminescent (PL) properties of the ancillary ligand Bpq are shown in Table 1. Ligand Bpq shows two absorption bands centered at 277 and 333 nm with molar extinction coefficients (ϵ) of $\sim 10^4$ (Table 1). In addition, Bpq displays an intense blue fluorescent emission, with a maximal emission wavelength

(28) (a) Fery-Forgues, S.; Le Bris, M.; Guetté, J.; Valeur, B. *J. Phys. Chem.* **1988**, *92*, 6233–6237. (b) Gans, P.; Sabatini, A.; Vacca, A. *Talanta* **1996**, *43*, 1739–1753.

(29) Frisch, M. J.; Trucks, G. W.; Schlegel, H. B.; Scuseria, G. E.; Robb, M. A.; Cheeseman, J. R.; Montgomery, J. A.; Vreven, T.; Kudin, K. N.; Burant, J. C.; Millam, J. M.; Iyengar, S. S.; Tomasi, J.; Barone, V.; Mennucci, B.; Cossi, M.; Scalmani, G.; Rega, N.; Petersson, G. A.; Nakatsuji, H.; Hada, M.; Ehara, M.; Toyota, K.; Fukuda, R.; Hasegawa, J.; Ishida, M.; Nakajima, T.; Honda, Y.; Kitao, O.; Nakai, H.; Klene, M.; Li, X.; Knox, J. E.; Hratchian, H. P.; Cross, J. B.; Bakken, V.; Adamo, C.; Jaramillo, J.; Gomperts, R.; Stratmann, R. E.; Yazyev, O.; Austin, A. J.; Cammi, R.; Pomelli, C.; Ochterski, J. W.; Ayala, P. Y.; Morokuma, K.; Voth, G. A.; Salvador, P.; Dannenberg, J. J.; Zakrzewski, V. G.; Dapprich, S.; Daniels, A. D.; Strain, M. C.; Farkas, O.; Malick, D. K.; Rabuck, A. D.; Raghavachari, K.; Foresman, J. B.; Ortiz, J. V.; Cui, Q.; Baboul, A. G.; Clifford, S.; Cioslowski, J.; Stefanov, B. B.; Liu, G.; Liashenko, A.; Piskorz, P.; Komaromi, I.; Martin, R. L.; Fox, D. J.; Keith, T.; Al-Laham, M. A.; Peng, C. Y.; Nanayakkara, A.; Challacombe, M.; Gill, P. M. W.; Johnson, B.; Chen, W.; Wong, M. W.; Gonzalez, C.; Pople, J. A. *Gaussian 03*, revision C.02; Gaussian, Inc.: Wallingford, CT, 2004.

(30) Hu, Y. Z.; Zhang, G.; Thummel, R. P. *Org. Lett.* **2003**, *5*, 2251–2253.

(31) Stahl, R.; Lambert, C.; Kaiser, C.; Wortmann, R.; Jakober, R. *Chem.—Eur. J.* **2006**, *12*, 2358–2370.

(32) Lamansky, S.; Djurovich, P.; Murphy, D.; Abdel-Razzaq, F.; Lee, H. E.; Adachi, C.; Burrows, P. E.; Forrest, S. R.; Thompson, M. E. *J. Am. Chem. Soc.* **2001**, *123*, 4304–4312.

(33) Nonoyama, K. *Bull. Chem. Soc. Jpn.* **1974**, *47*, 467.

Table 1. Photophysical Properties of Bpq and $[Ir(Bpq)_2(bpy)]^+PF_6^-$ Measured in a CH_3CN Solution[a]

compound	λ_{abs} (log ϵ) (nm)	λ_{em} (nm)	Φ_{em}	τ (μs)
Bpq	277 (4.46), 333 (4.56)	439	0.51	
$[Ir(Bpq)_2(bpy)]^+PF_6^-$	289 (4.84), 351 (4.73), 368 (4.65), 465 (3.77)	592, 637 (sh)	0.49	2.67

[a] The solution was degassed by three freeze−pump−thaw cycles.

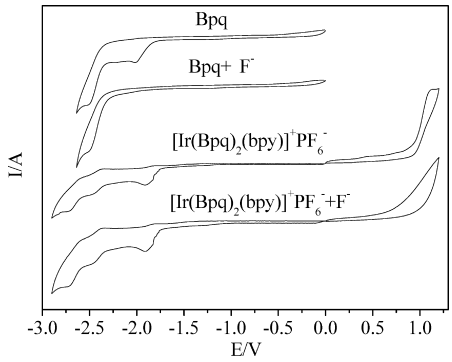

Figure 1. Cyclic voltammograms of Bpq and $[Ir(Bpq)_2(bpy)]^+PF_6^-$ before and after the addition of F^-.

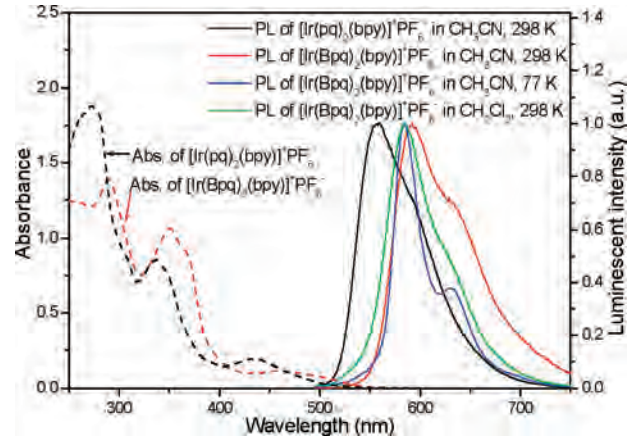

Figure 2. Absorption and PL spectra of $[Ir(Bpq)_2(bpy)]^+PF_6^-$ (20 μM) and $[Ir(pq)_2(bpy)]^+PF_6^-$ in different conditions. The solution was degassed by three freeze−pump−thaw cycles.

at 439 nm. As shown in Figure 1, Bpq shows two reduction waves at −2.01 and −2.50 V.

Electrochemical Properties of $[Ir(Bpq)_2(bpy)]^+PF_6^-$. The electrochemical properties of $[Ir(Bpq)_2(bpy)]^+PF_6^-$ were studied by cyclic voltammetry. As shown in Figure 1, $[Ir(Bpq)_2(bpy)]^+PF_6^-$ exhibits an irreversible oxidation wave. In addition, $[Ir(Bpq)_2(bpy)]^+PF_6^-$ exhibits three reduction waves at −1.90, −2.46, and −2.72 V. According to a previous report,[34] the waves at −2.46 and −2.72 V are assigned to the reduction of pq fragments. Also, according to previous reports on cationic iridium(III) complexes containing bpy,[35] we tentatively assign the wave at −1.90 V to reduction of the bpy ligand.

Photophysical Properties of $[Ir(Bpq)_2(bpy)]^+PF_6^-$. To better understand the photophysical properties of $[Ir(Bpq)_2(bpy)]^+PF_6^-$, DFT calculations for this complex were performed and molecular orbitals were studied (see Figure 3). The HOMO distribution primarily resides on the $BMes_2$ fragments of ligand Bpq. Also, the HOMO−2 distribution resides on the iridium center and phenyl groups of ligand Bpq. HOMO−6 and HOMO−3 distributions are located at the iridium center and $BMes_2$ fragments of Bpq. In addition, the LUMO distribution is dominated by the ligand bpy, and LUMO+2 distribution is located at the Bpq ligand.

Time-dependent DFT (TDDFT) calculations were then performed to estimate the corresponding transition energy of complex $[Ir(Bpq)_2(bpy)]^+PF_6^-$. The calculated parameters for the lowest-lying transitions are listed in Table 2. The lowest triplet state originates from HOMO−6 → LUMO, HOMO−3 → LUMO, HOMO−2 → LUMO, and HOMO−2 → LUMO+2, which apparently possess a mixture of [$\pi_{C\wedge N} \rightarrow \pi^*_{N\wedge N}$] ^{3}LLCT and [$d\pi(Ir) \rightarrow \pi^*_{N\wedge N}$] ^{3}MLCT transitions with some contribution from ^{3}LC ($\pi_{C\wedge N} \rightarrow \pi^*_{C\wedge N}$). Hence, the weak absorption bands in the range of 400−600 nm can be assigned to a mixture of ligand-to-ligand charge transfer (LLCT), metal-to-ligand charge transfer (MLCT), and spin-forbiden ligand-centered (^{3}LC) transitions. The $BMes_2$ groups play a significant role in the excited state of $[Ir(Bpq)_2(bpy)]^+PF_6^-$.

$[Ir(Bpq)_2(bpy)]^+PF_6^-$ shows an intense emission band at 592 nm with a shoulder at 637 nm, and the PL color is orange-red at room temperature in a CH_3CN solution. The phosphorescence quantum yield in degassed solution is 0.49 and that in an aerated solution is 0.17 measured by a calibrated integrating sphere system, indicating that the emission is sensitive to oxygen. The moderately high phosphorescence quantum yield (0.17) in an aerated solution ensures that this complex can function as a phosphorescence fluoride ion sensor. The emission lifetimes and excitation spectra monitored at 592 and 637 nm are almost the same (see Table 1), indicating that the two bands relate to the same excited state. The PL spectrum of $[Ir(Bpq)_2(bpy)]^+PF_6^-$ is broad and featureless, and thus it can be concluded that the emission of $[Ir(Bpq)_2(bpy)]^+PF_6^-$ primarily originates from CT states. Upon comparison with the model complex $[Ir(pq)_2(bpy)]^+PF_6^-$, it is seen that the emission wavelength of $[Ir(Bpq)_2(bpy)]^+PF_6^-$ is significantly red-shifted, suggesting that the $BMes_2$ group makes a significant contribution to the excited state of $[Ir(Bpq)_2(bpy)]^+PF_6^-$.

PL spectra of $[Ir(Bpq)_2(bpy)]^+PF_6^-$ in different solvents and at different temperatures were also measured (Figure 2). A blue shift of the emission maximum was observed from a fluid solution at room temperature to a rigid matrix at 77 K, which is often observed for cyclometalated iridium(III) diimine MLCT and LLCT emitters.[36] The blue shift is caused by fast solvent reorganization in a fluid solution at room temperature, which can stabilize the CT states before emission takes place. At 77 K, however, this stabilization

(34) Wu, F. I.; Su, H. J.; Shu, C. F.; Luo, L.; Diau, W. G.; Cheng, C. H.; Duan, J. P.; Lee, G. H. *J. Mater. Chem.* **2005**, *15*, 1035–1042.
(35) Neve, F.; La Deda, M.; Crispini, A.; Bellusci, A.; Puntoriero, F.; Campagna, S. *Organometallics* **2004**, *23*, 5856–5863.
(36) Juris, A.; Balzani, V.; Barigelletti, F.; Campagna, S.; Belser, P.; von Zelewsky, A. *Coord. Chem. Rev.* **1988**, *84*, 85–277.

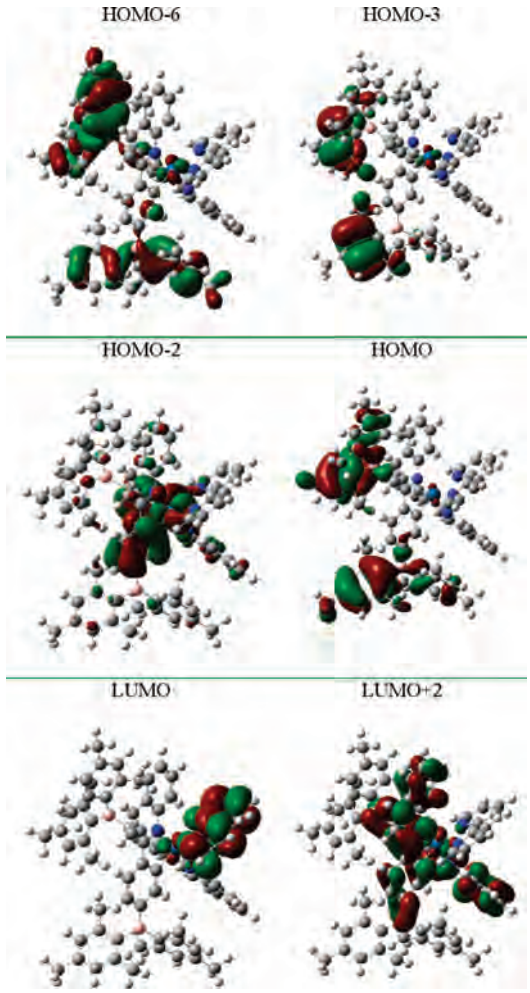

Figure 3. HOMO−6, HOMO−3, HOMO−2, HOMO, LUMO, and LUMO+2 distributions of $[Ir(Bpq)_2(bpy)]^+PF_6^-$.

Table 2. Calculated Energy Levels of the Lowest Singlet (S_1) and Triplet States (T_1) for $[Ir(Bpq)_2(bpy)]^+PF_6^-$

state	excitation	E_{cal}[a] (eV)	λ_{cal} (nm)	f[b]
S_5	HOMO−6 → LUMO+2 (11%) HOMO−2 → LUMO+2 (67%)	2.53	490	0.0456
T_1	HOMO−6 → LUMO (11%) HOMO−3 → LUMO (10%) HOMO−2 → LUMO (67%) HOMO−2 → LUMO+2 (10%)	2.08	596	0

[a] E_{cal}: calculated energy. [b] f: calculated oscillator strength.

of CT states is hampered. PL measurement in different solvents revealed that the emission maximum of $[Ir(Bpq)_2(bpy)]^+PF_6^-$ occurs at higher energy in the less polar CH_2Cl_2 than in the more polar CH_3CN (Figure 2), which is also very common for cyclometalated iridium(III) diimine MLCT and LLCT emitters. Hence, the excited state of $[Ir(Bpq)_2(bpy)]^+PF_6^-$ can be assigned to a CT state.

Recently, Marder et al. have reported a neutral iridium(III) complex Ir−B with a $B(Mes)_2$ group on the C∧N ligand (2-phenylpyridine).[18g] Compared with the complex without a $B(Mes)_2$ group, an evident red shift in the emission wavelength can be observed, which is similar to our complex $[Ir(Bpq)_2(bpy)]^+PF_6^-$. In addition, both Ir−B and $[Ir(Bpq)_2(bpy)]^+PF_6^-$ exhibit red emission and the emission originates from the CT state. In addition, Wang et al. also reported a copper(I) complex and a platinum(II) complex

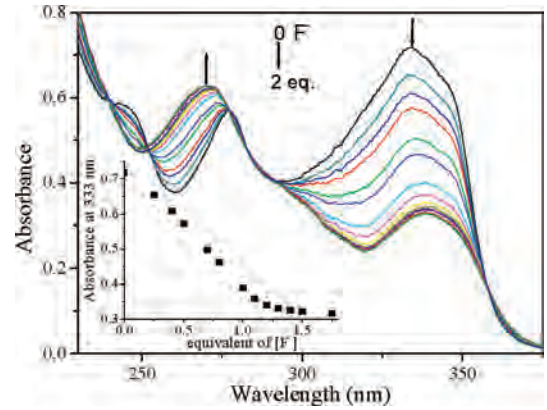

Figure 4. Change in the UV−vis absorption spectra of Bpq (20 μM) in a CH_3CN solution with various amounts of F^-. Inset: absorption titration profile at 333 nm versus 1 equiv of F^- in solution for Bpq.

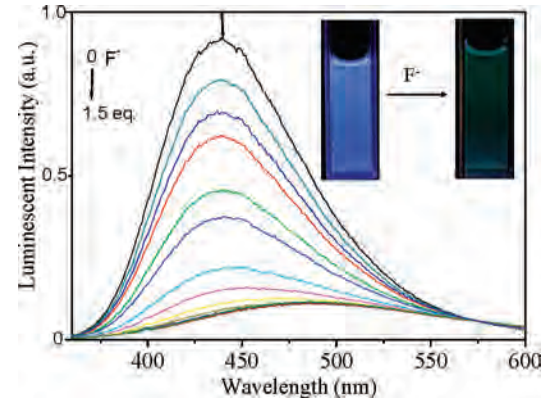

Figure 5. Change in the emission spectra of Bpq (20 μM) in a CH_3CN solution with various amounts of F^- (λ_{ex} = 358 nm). Inset: emission color observed in a CH_3CN solution of Bpq (500 μM) in the absence (left) and presence (after) of 1 equiv of F^-.

with a $B(Mes)_2$ group in the ligand. Both complexes have longer emission lifetimes and lower quantum yields in solution compared with $[Ir(Bpq)_2(bpy)]^+PF_6^-$.[8d]

Optical and Electrochemical Responses of Bpq to F^-. It has been demonstrated that the vacant p orbital on the boron atom in the triarylborane derivative coordinates selectively with fluoride anions, giving rise to changes in both the absorption and emission spectra of the triarylborane derivative. In the present study, the ability of Bpq to complex with F^- was investigated using UV−vis absorption and emission titration experiments. After the addition of F^-, the absorption band at 333 nm was red shifted (see Figure 4). As shown by absorption and emission titration curves, Bpq needs approximately 1 equiv of F^- to reach saturation. The binding constant (K) was calculated to be 4.70×10^4 M^{-1} from the absorption titration curve. Furthermore, the addition of F^- induces an obvious variation in the electrochemical properties of Bpq (Figure 1). Taken together, these experimental results indicate an intense interaction between the boron center and the fluoride anion.

Importantly, the addition of F^- caused a decrease in the emission intensity and a red shift of the emission band from 439 to 485 nm (Figure 5), corresponding to a visual change in the emission color from bright blue to weak blue-green (Figure 5, inset). In many previous reports,[6−11] coordination of fluoride to the empty p orbital of the boron atom would

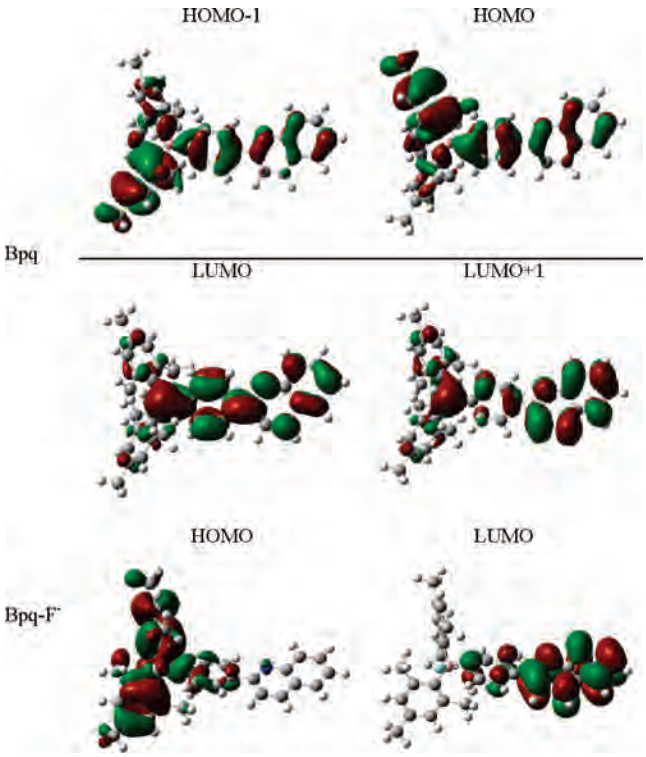

Figure 6. Orbital distributions of Bpq and Bpq-F^-.

block intramolecular CT or interrupt the π conjugation extended through the boron atom, which led to fluorescence quenching or a dramatic blue shift of the emission bands. In this case, however, we observed a red shift of emission spectra induced by complexation with F^-. According to the calculation results (see below), the complexation with F^- switches the excited state from the $\pi-\pi^*$ transition of Bpq to the CT transition of the adduct Bpq-F^-, which is different from many other reports. Also, it is this switch of the excited state that leads to the red shift of the emission spectra. A similar switch of the excited state has also been reported by DiCesare and Lakowicz[11i] and Spange et al.[11n] In these systems, boronic acid (or boranate ester) groups, which act as electron-withdrawing groups, were used as binding sites for F^-. Upon complexation with F^-, they can be changed into electron-donating groups. When these groups and other electron-withdrawing groups were introduced into the same π-electron system, the complexation with F^- could induce CT interaction between the anionic boron acid (or boronate) ester and the electron-withdrawing groups.

Moreover, a very weak variation in the absorption and emission spectra of Bpq was observed upon the addition of an excess of other anions, such as Br^-, Cl^-, I^-, ClO_4^-, NO_3^-, CH_3COO^-, and $H_2PO_4^-$ (see the Supporting Information), indicating that Bpq displays high selectivity in sensing F^-.

Mechanism of the Bpq Response to F^-. To understand the mechanism by which Bpq responds to F^-, molecular orbital calculations for Bpq and the adduct Bpq-F^- were performed using TDDFT calculations (see Figure 6 and Table 3). For Bpq, the $BMes_2$ group and the quinoline (pq) segment have a planar arrangement. The HOMO−1 and HOMO distributions of Bpq are predominantly located on the mesityl group and the pq unit. The LUMO is localized on the boron center and the pq unit, so the first reduction wave of Bpq is tentatively assigned to the reduction of the boron center and the pq unit. The LUMO+1 orbital is mainly localized on the pq fragment with some distribution on the boron center. So, the second reduction wave of Bpq was tentatively assigned to the reduction of the pq fragment with some contribution from the boron center. The lowest singlet state originates from HOMO−1 → LUMO, HOMO → LUMO, and HOMO → LUMO+1 (see Table 3). So, the lowest electronic transition in Bpq can mainly be attributed to the $\pi-\pi^*$ transition of Bpq with CT from the mesityl group to the pq unit. Compared to Bpq, evident variation in the molecular orbital distributions is observed for the adduct Bpq-F^-. The HOMO distribution is located on the $BMes_2$ unit, and the LUMO distribution resides on the pq unit. The lowest electronic transition originates from HOMO → LUMO. These facts indicate that the lowest electronic transition of Bpq-F^- can be attributed to CT from $BMes_2$ to the pq unit. Hence, after complexation with F^-, the excited state is switched from the $\pi-\pi^*$ transition of Bpq to the CT transition, resulting in variation in the photophysical and electrochemical properties of Bpq. In addition, surface charge analysis based on DFT indicates that the charge on the boron atom after binding of F^- increased significantly compared with that before binding of F^- (Supporting Information), which also shows a reversal of the roles of the acceptor and donor for the boron atom upon F^- binding.

Table 3. Calculated Energy Levels of the Lowest Singlet (S_1) for Bpq and Bpq-F^-

state	excitation	E_{cal}[a] (eV)	λ_{cal} (nm)	f[b]
Bpq	HOMO−1 → LUMO (42%) HOMO → LUMO (53%) HOMO → LUMO+1 (11%)	3.39	366	0.0627
Bpq-F^-	HOMO → LUMO (70%)	2.81	441	0.0419

[a] E_{cal}: calculated energy. [b] f: calculated oscillator strength.

Optical Responses of $[Ir(Bpq)_2(bpy)]^+PF_6^-$ to F^-. Considering the significant response of ligand Bpq to F^-, it is reasoned that the photophysical and electrochemical properties of $[Ir(Bpq)_2(bpy)]^+PF_6^-$ could be affected upon the addition of F^-. Figure 7 shows the variation in the absorption spectra of $[Ir(Bpq)_2(bpy)]^+PF_6^-$ upon the addition of F^-. When F^- was added to a solution of $[Ir(Bpq)_2(bpy)]^+PF_6^-$, the absorbance at 290 and 350 nm decreased gradually whereas the absorbance at 400 nm increased, corresponding to an isobestic point at 379 nm. Importantly, the absorption band in the range of 420−600 nm was red-shifted with an increase in the absorbance, corresponding to a change in the solution color from yellow to orange-red (Figure 7, inset), indicating that $[Ir(Bpq)_2(bpy)]^+PF_6^-$ can serve as a "naked-eye" indicator of F^-.

As shown in Figure 8, emission spectra of $[Ir(Bpq)_2(bpy)]^+PF_6^-$ also displayed obvious changes when F^- was added. A decrease in the emission intensity of $[Ir(Bpq)_2(bpy)]^+PF_6^-$ was observed upon the addition of F^-. After the addition of approximately 2 equiv of F^-, the emission of $[Ir(Bpq)_2(bpy)]^+PF_6^-$ was almost completely quenched, which could be observed by the naked eye (Figure 9). Hence,

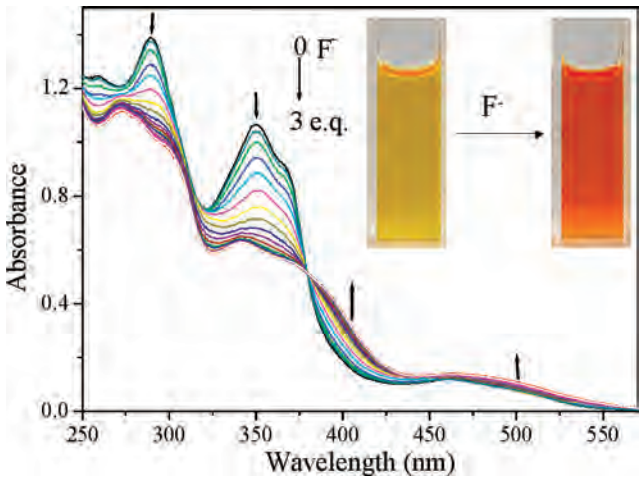

Figure 7. Change in the UV−vis absorption spectra of $[Ir(Bpq)_2(bpy)]^+PF_6^-$ (20 μM) in a CH_3CN solution with various amounts of F^-. Inset: solution color observed in a CH_3CN solution of $[Ir(Bpq)_2(bpy)]^+PF_6^-$ (500 μM) in the absence (left) and presence (after) of 2 equiv of F^-.

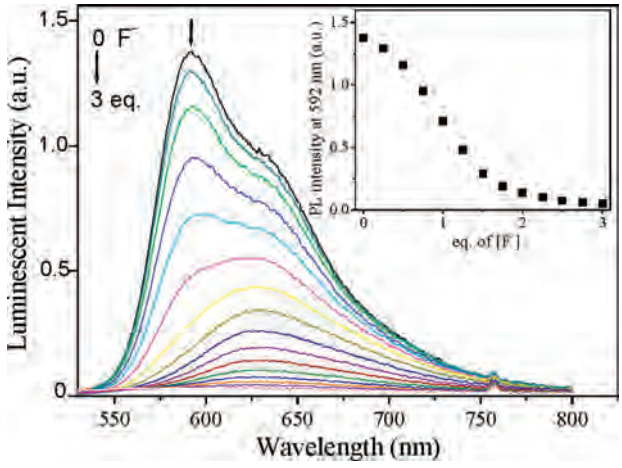

Figure 8. Change in the emission spectra of $[Ir(Bpq)_2(bpy)]^+PF_6^-$ (20 μM) in an air-equilibrated CH_3CN solution with various amounts of F^- (λ_{ex} = 379 nm). Inset: fluorescent titration profile at 592 nm versus 1 equiv of F^- in solution for $[Ir(Bpq)_2(bpy)]^+PF_6^-$.

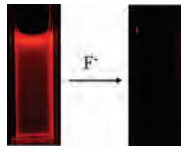

Figure 9. Emission color observed in a CH_3CN solution of $[Ir(Bpq)_2(bpy)]^+PF_6^-$ (500 μM) in the absence (left) and presence (right) of 2 equiv of F^-.

$[Ir(Bpq)_2(bpy)]^+PF_6^-$ could be used as an ON−OFF-type phosphorescent probe for F^-.

Considering that there are two boron centers in one complex molecule, it is possible for $[Ir(Bpq)_2(bpy)]^+PF_6$ to form a 1:2 complex with 2 equiv of F^-. This has been verified by variation in the ^{11}B NMR spectra of $[Ir(Bpq)_2(bpy)]^+PF_6$ before and after the addition of F^- (see Figure S7 in the Supporting Information). After complexation with F^-, the signal was changed completely, suggesting that both of the two boron centers in the complex bind with F^-. Using the UV−vis titration data, the binding constants K_1 and K_2 of $[Ir(Bpq)_2(bpy)]^+PF_6$ with F^- were determined to be 1.29×10^6 and 4.27×10^5 M^{-1}, respectively.

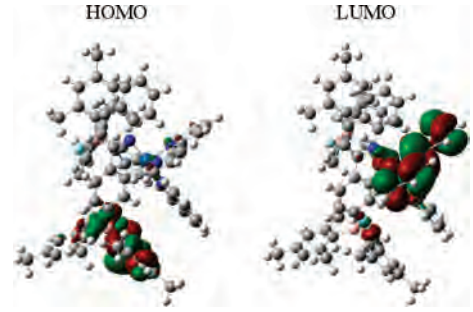

Figure 10. HOMO and LUMO distributions of $[Ir(Bpq)_2(bpy)]^+PF_6^-$-$2F^-$.

Table 4. Calculated Energy Levels of the Lowest Singlet (S_1) and Triplet States (T_1) for $[Ir(Bpq)_2(bpy)]^+PF_6^-$-$2F^-$

state	excitation	f^a
S_1	HOMO → LUMO	0.0045
T_1	HOMO → LUMO	0

[a] *f*: calculated oscillator strength.

Molecular orbital calculations for the adduct $[Ir(Bpq)_2(bpy)]^+PF_6^-$-$2F^-$ were performed using TDDFT calculations (see Figure 10 and Table 4). HOMO distribution resides on the $BMes_2$-F^- fragments. Also, LUMO distribution resides on the bpy fragment. The lowest triplet state originates from HOMO → LUMO, which shows that the complexation of $BMes_2$ with F^- changes the exicited-state property of the complex.

The influence of F^- on the electrochemical properties of $[Ir(Bpq)_2(bpy)]^+PF_6^-$ was also investigated. Upon the addition of F^-, the oxidation wave disappeared. The reason for the disappearance of the oxidation wave is not very clear. For $[Ir(Bpq)_2(bpy)]^+PF_6^-$, the HOMO distribution resides on the $BMes_2$ fragment, so the irreversible oxidation process of $[Ir(Bpq)_2(bpy)]^+PF_6^-$ can be tentatively assigned to the oxidation of $BMes_2$ groups. After complexation with F^-, the HOMO distribution resides on the $BMes_2$-F^- fragment. So, the disappearance of the oxidation wave of $BMes_2$ groups can be tentatively attributed to the formation of a $BMes_2$-F adduct, which prevents the oxidation of $BMes_2$ groups.

High selectivity is necessary for an excellent chemosensor. Herein, the selective coordination studies of $[Ir(Bpq)_2(bpy)]^+PF_6^-$ by absorption and emission spectra were then extended to other anions in a CH_3CN solution. As shown in Figure 11, only the addition of F^- results in prominent changes in the ratio of absorbance at 350 and 400 nm, whereas the addition of a large excess of other anions (such as Cl^-, Br^-, I^-, ClO_4^-, NO_3^-, $H_2PO_4^-$, and CH_3COO^-) causes slight changes. Therefore, $[Ir(Bpq)_2(bpy)]^+PF_6^-$ displayed a high selectivity in sensing F^-. Achieving high selectivity for the analyte of interest over a complex background of potentially competing species is a challenge in sensor development. Thus, the competition experiment was also carried out by the addition of F^- to solutions of $[Ir(Bpq)_2(bpy)]^+PF_6^-$ in the presence of other anions. As shown in Figure 11, whether in the absence or presence of other anions, obvious spectral changes were observed for $[Ir(Bpq)_2(bpy)]^+PF_6^-$ upon the addition of F^-. The results indicate that the sensing of F^- by $[Ir(Bpq)_2(bpy)]^+PF_6^-$ is hardly affected by these commonly coexistent ions. Therefore, $[Ir(Bpq)_2(bpy)]^+PF_6^-$ can

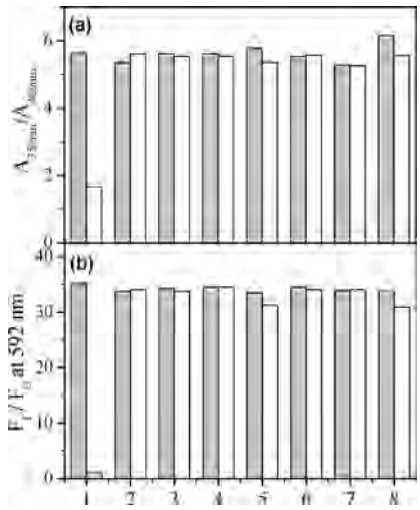

Figure 11. Absorption (a) and fluorimetric (b) responses of $[Ir(Bpq)_2(bpy)]^+PF_6^-$ (20 μM) in the presence of 2 equiv of F^- or 5 equiv of other anions in a MeCN solution. Bars represent the ratio $A_{350\ nm}/A_{400\ nm}$ of the absorbance intensity at 350 and 400 nm (a) and the emission intensity ($I_{592\ nm}$) at 592 nm (b). Gray and white represent $A_{350\ nm}/A_{400\ nm}$ and $I_{592\ nm}$ before and after the addition of anions, respectively. Bars: 1, F^-; 2, Cl^-; 3, Br^-; 4, I^-; 5, ClO_4^-; 6, NO_3^-; 7, $H_2PO_4^-$; 8, CH_3COO^-.

act as a highly selective phosphorescent chemosensor for F^-. It should be pointed out that all systems containing $BMes_2$ groups that have been examined as fluoride ion sensors are ion specific and that some workers have also commented on their CN^- binding affinities.[12d]

Conclusion

In summary, we have synthesized a new iridium(III) complex $[Ir(Bpq)_2(bpy)]^+PF_6^-$ containing bismesitylboryl groups. The investigation of the photophysical and electrochemical properties of ligand Bpq and complex $[Ir(Bpq)_2(bpy)]^+PF_6^-$ shows that they can be used as highly selective chemosensors for F^- detectable by the naked eye. The dimesitylboryl group is believed to play very important roles in these unique responses. For the cyclometalated ligand Bpq, an evident red shift of the emission spectra was observed after the addition of F^-. This variation can be explained by the excited-state switch from $\pi-\pi^*$ to CT transition. For $[Ir(Bpq)_2(bpy)]^+PF_6^-$, the addition of F^- induces an evident change in the solution color from yellow to orange-red and a pronounced ON−OFF-type phosphorescent signaling behavior. Hence, $[Ir(Bpq)_2(bpy)]^+PF_6^-$ can act as an excellent phosphorescent chemosensor for F^- with naked-eye detection. This work provides a useful design strategy for the synthesis of new phosphorescent chemosensors by simple modification of the chemical structure of ligands to contain a specific recognition site.

Acknowledgment. The authors are thankful for financial support from National Natural Science Foundation of China (Grants 20490210, 20501006, and 20775017), NHTPC (Grant 2006AA03Z318), NCET-06-0353 and Shanghai Science and Technology Community (Grant 06QH14002), Huo Yingdong Education Foundation (Grant 104012), and Shanghai Leading Academic Discipline Project (Project B108).

Supporting Information Available: Excitation spectra of $[Ir(Bpq)_2(bpy)]^+PF_6^-$, UV−vis and fluorescence spectra of Bpq and $[Ir(Bpq)_2(bpy)]^+PF_6^-$ upon titration with other anions, selective absorption and fluorimetric response of Bpq to various anions, and surface charge distributions of Bpq and Bpq-F^-. This material is available free of charge via the Internet at http://pubs.acs.org.

IC800500C